Tribology Letters (2020) 68:124
https://doi.org/10.1007/s11249-020-01362-1

ORIGINAL PAPER

Tribological Investigations of Nano and Micro-sized Graphite Particles as an Additive in Lithium-Based Grease

Nikhil Kumar[1,2] · Vinay Saini[1] · Jayashree Bijwe[1]

Received: 31 July 2020 / Accepted: 19 October 2020 / Published online: 6 November 2020

Abstract
Graphite is a well-known solid lubricant (SL) additive widely used both as a standalone SL and also as additive in lubricating oils, greases, composites, etc. Size of the additive particles especially nano-particles (NPs) is a major attribute to the performance properties of a composite, oil, grease, etc. This paper highlights the influence of graphite particles of four sizes viz. 50 nm, 450 nm, 4 microns and 10 microns incorporated in the grease in identical amount (4 wt. %) on the anti-friction (AF), anti-wear (AW) and extreme-pressure (EP) performance. The results indicated that all sizes proved beneficial for all the selected properties. Higher the size of particles, lower was the improvement in performance. The particles were most effective as anti-friction additive (AFA) followed by anti-wear additive (AWA) and then extreme-pressure additive (EPA). The NPs exhibited highest improvement as AFA (57%), AWA (41%) and EPA (25%). Raman Spectroscopy proved the formation of exfoliated graphitic layer on the worn surface of balls. Furthermore, SEM micrograph with elemental mapping and XPS spectroscopy analysis proved supportive in comprehending the mechanisms responsible for improved tribo-performance.

Keywords Graphite particles · Lithium grease · Anti-wear additive (AWA) · Anti-friction additive(AFA) · Nano-grease

1 Introduction

Friction is the prime source of energy consumption in various industrial equipment of various sectors such as manufacturing, power transmission and transportation [1]. Undesirable friction between relative moving parts might lead to gradual wear and thus massive losses (5–7%) to gross national product of developed countries [2]. Lubrication of surfaces is vital for the tribo-components to reduce friction, energy losses and wear, apart from increasing their efficiency. Novel lubricants and grease are likely to play a substantial role by improving fuel efficiency, reducing emissions and extending the service life of machines [3–7]. Grease is one of the most intriguing forms of the lubricants with distinct advantages such as leak-resistance, non-dripping and sealing property and more importantly the capability to hold both nano- and micro-meter-sized additive particles in suspended form. This capability opens up the doors of formulating nano-greases efficiently with least possibility of agglomeration and sedimentation of nano-particles (NPs). Some solid lubricants (SLs) such as PTFE [8–10], MoS_2 [11], graphite [12, 13], etc., have previously been shown as effective additives in grease formulations. Other lesser known SLs such as Talc [14], CaF_2 crystals [15], $CaCO_3$ [16], copper powder [17] and copper oxide [18] have shown some potential as anti-wear (AW), anti-friction (AF) and enhanced load-carrying capacity either alone or in combination. Carbon in various forms viz. crystalline as graphite [12, 13], 2D structure as graphene [19] or multilayer graphene (MLT) [20] and tubular form as carbon nanotubes (CNTs) [21] etc. has shown significant potential to influence the AF, AW and Extreme Pressure (EP) properties of lubricating greases (Table 1).

The size of SLs also impacts the rheological and tribological properties of greases [13, 26, 27]. Niu and Qu [13] studied the effect of different sized graphite nanosheet of (Día 2, 3.5, 6 μm) in titanium complex grease and reported that the smaller-sized nanosheet of 2 μm benefitted most by showing 14% improvement in AF and 2% improvement in AW performance compared to the base grease. Interestingly,

✉ Jayashree Bijwe
jbijwe@gmail.com

1 Centre for Automotive Research and Tribology (CART), (Formerly ITMMEC), Indian Institute of Technology, Delhi 110016, India

2 Current Address: Bharat Petroleum Corporation Limited, R&D Centre, Mumbai 400015, India

Table 1 Literature on the performance of greases with Carbonaceous fillers

S No. Ref.	Soap/base	Solid additive Size % wt.	Mixing technique	Evaluation Techniques	Finding
1 [12]	G [1 µm/15%] Clay [2.5, 5 and 7.5] and Li St. [4.8 and 12%]	• DBDS, TCP and Cereclor • 1.7%	G: Rotary evaporator; Clay; and Li St: stirrer and colloidal mill	UMT; DP, PT	EP: Graphite grease> lithium grease> clay grease
2 [13]	Titanium complex (15%)/150BS + 350SN (1:4)	• G • Dia−2 µm, 3.5 µm and 6 µm/ Thickness- 20–40 nm • 0.8, 1.0 and 1.2%	Mechanical stirring and three-roller grinding	4-ball tester for AW and EP; DP, PT; SEM; XPS	µ: $G_{2\mu m}$ (15% ↓) > $G_{3.5\mu m}$ (14% ↓) > $G_{6\mu m}$ (13% ↓) > BG WSD: $G_{2\mu m}$ (3% ↓) > $G_{3.5\mu m}$ (2% ↓) > $G_{6\mu m}$ (2% ↓) > BG optimum %: $G_{2\mu m}$ (0.8%); $G_{3.5\mu m}$ (1%); $G_{6\mu m}$ (1.2.%)
3 [19]	Li St.	• G, Graphene and GO • 1%	Sonication in benzene	XRD: TEM; 4-ball wear and EP	µ: Graphene (50%↓) > > GO (30% ↓) > G WSD: Graphene (61%↓) > GO (56%↓)> G (480 µm)
4 [20]	Bentonite/ PAO 40	• MLG; 0.1% • G-5%	PAO 40 + bentone (+ acetone) +MLG (+ ethanol)	DP, PT, TGA SRV, Micro XAM-3D SMM, SEM and TEM	μ_{min} – with 0.1% MLG μ_{min} (0.1% MLG) <μ_{min} (5% G) WV $_{min}$ MLG @ all loads EP (500 N) and µ (0.15) @ 150 ^{0}C
5 [21]	Li St/ PAO	• CNT • D-10 nm/L-5 µm • 1%	Chloroform as solvent	TEM: XRD: SEM: 4-ball wear and EP	µ: CNT (82% ↓) > BG WSD: CNT (63% ↓) > BG EP: CNT (52% ↑) > BG
6 [22]	G (90%)/Oil	–	–	DP, PT	µ: activated G (120–150%) > G
7 [23]	Li St (14%)/Paraffin oil	• Inter-lamellar spacing: GO (0.81 nm), rGO (0.35 nm) and GO-ODA (0.42 nm) • 0.01–0.05 wt.%	Mechanical stirring	4-ball wear and EP; FTIR, TEM; SEM-EDS	µ: rGO (50% ↓) > GO (34% ↓) > GO ODA (34% ↓) > BG WSD: GO (37% ↓) > rGO (36% ↓) > GO ODA (32% ↓) > BG WV: GO (87% ↓) > rGO (86% ↓) > GO ODA (81% ↓) > BG
8 [24]	Lithium, calcium, sodium, Li-Ca grease	Commercial EP additive, graphite, MoS_2, and carbon black	Mechanical stirring	4-ball wear and EP; DP, PT	1.5% EP additive ~3% G~ 1% MoS_2~ 2.5% carbon black
9 [25]	Li St	FLG 0, 0.05, 0.10 and 0.20 wt.%)	Mechanical stirring + sonication + grinding in 3-roll grinder	4-ball wear, AFM, Raman, SEM-EDS, XPS	Optimum dosage of FLG-0.1% µ-at 686N: FLG (22.3%↓) > BG µ-at 600rpm: FLG (15.5%↓) > BG

G graphite, *Li St.* lithium stearate, *µ* coefficient of friction, *DBDS* Dibenzyl disulphide, *UMT* universal mechanical tester, *PT* pour point test, *DP* penetration test, *CNT* Carbon nanotube, *MLG* multilayer graphene GO-graphene oxide, *XRD* X-ray crystallography, *TEM* transmission electron microscopy, *WSD* wear scar dia, *WV* wear volume, *rGO* reduced graphene oxide, *GO ODA* Octadecylamine functionalized graphene oxide, *PAO* Poly-alpha olefins, *TGA* thermo-gravimetric analysis, *SEM* scanning electron microscopy, *EDS* energy dispersive X-Ray spectroscopy, *FLG* few layer graphene, *AFM* atomic force microscopy the variation of morphology plays an important role on the tribological performance [28]. Kumar et al. [26] reported the effect of size and shape of PTFE particles on grease performance and reported that bigger the size of PTFE particles, lower is its potential to enhance the AF, AW and EP performance of a grease. Compared to the virgin grease, spherical micro-particles (MPs) of PTFE showed 76% higher benefits while NPs of cylindrical shape exhibited 61% [26]. Gupta et. al. [27] have reported the effect of graphite of various sizes with dispersant in oil. The research efforts on the exploration of MPs and NPs of graphite in greases [12, 13, 19, 22, 24] showed that no studies could be available on the size and performance correlation effect for all the tribo-performance properties such as AF, AW and EP. Keeping this in view, four sizes of graphite particles (50 nm, 450 nm, 4 µm and 10 µm) in a fixed amount (4 wt.%) were selected to develop greases to examine the effect as AFA, AWA and EPA and the investigations along with analysis are stated in the following sections.

2 Experimental Details

2.1 Materials

Lithium-based soap used for formulations of grease was developed through saponification process employing LiOH (Lithium Hydroxide) and 12-HSA (Hydroxystearic Acid). The specifications of selected chemicals for formulations of pristine grease are shown in Table 2. Details of various sizes of graphite particles selected as additive are shown in Table 3.

2.2 Grease Synthesis Procedure

Grease were prepared through standard process by means of a grease kettle, agitator and stirrer. Selected NPs and MPs with 4 wt. % dosage were uniformly dispersed in Poly-alpha olefin (PAO) oils using probe sonication for 60 minutes. Then dispersed graphite particles in PAO were instantly added to grease soap. Finally, the grease mixed with graphite particles was homogenized for twenty minutes using a cylindrical roller mill. The detailed synthesis procedure of lithium grease is reported in the earlier paper [26]. Fourier-transform infrared spectroscopy (FTIR) analysis established the presence of Lithium stearate (Fig. 1). All grease samples were formulated using soap having 20 wt. % dosing of thickening agent.

2.3 Particle Size Characterization

The size and shape of Graphite particles were confirmed through Scanning electron microscopy (SEM) using (EVO 10, Carl Zeiss) and Transmission electron microscopy (TEM). The distribution of NPs in formulated nano-grease was evaluated through Cryo-SEM make JIB-4700F. For sample preparation, the frozen oil drop was 'etched' to reveal more details and then was finally coated with platinum by sputtering [26]. The 5kV source was used to avoid excess heat dissipation on the surface.

2.4 Characterization of Greases

The drop point and consistency of formulated nano-grease was calculated using standard drop point tester and penetrometer apparatus. The particulars of each of method

Table 2 Materials used in pristine grease synthesis

Materials	PAO	12-HSA	LiOH
Specifications	–	Analytical reagent grade (>99%)	Analytical reagent grade
Source	Chevron Phillips Chemicals	TCI Chemicals (India)	SD Fine Chemicals (India)
Material	PAO	12-Hydroxystearic Acid	Lithium hydroxide (LiOH)

Table 3 Codes and designation assigned to different sized graphite particles doped in nano-greases

S No.	Particle size	Manufacturer	Graphite code	Formulated nano-grease (4 wt. %)
1	10 µm	Imerys Graphite and Carbon, Switzerland	G_B	G_{B4}
2	4 µm	Imerys Graphite and Carbon, Switzerland	G_M	G_{M4}
3	450 nm	Nanostructured and Amorphous Materials, Inc., USA	G_S	G_{S4}
4	50 nm	Nanostructured and Amorphous Materials, Inc., USA	G_N	G_{N4}

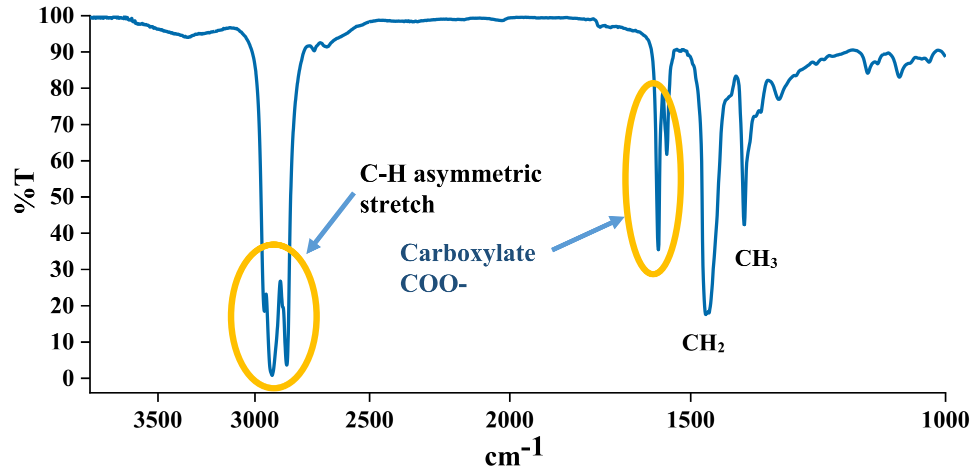

Fig. 1 FTIR peaks confirming the presence of lithium stearate grease [26]

employed along with its procedure used for characterization are discussed below in subsequent sections.

2.4.1 Consistency Measurement

The consistency is a measure of relative hardness of grease. The grease consistency is measured as the penetration of standard cone assembly through the grease surface in tenth of millimetres. In the present study, all the synthesized greases were subjected to penetration using one half cone method as per ASTM D1403 using Anton Paar PNR 12 penetrometer. This method is applied when small sample of lubricating greases is to be tested.

2.4.2 Drop-Point Measurement

The drop-point of lubricating grease is the measure of temperature at which the conventional soap thickener passes from semi-solid to liquid state underneath standard defined operating conditions. It is measured as per ASTM D2265 using Petrotest drop point tester and provides a direct correlation with the allowable operating temperature of the grease.

2.5 Tribo-Performance Evaluation

Three testing methods were incorporated to evaluate the tribo-performance of developed greases and nano-grease viz. UMT (Universal mechanical tester) for frictional behaviour, four-ball tester for wear and load-carrying capacity were employed. Each test was repeated thrice followed by averaging the values.

2.5.1 Anti-Friction (AF) Property Evaluation

Anti-friction property of greases was evaluated in reciprocating motion of ball on plate using UMT (Universal Mechanical Tester) supplied by CETR USA. The ball (0.375″ diameter of 52100 steel) reciprocated against lower test plate of same bearing steel material (60 Rc hardness and 0.45–0.65-µm surface finish, 24-mm diameter by 7.85 mm thick). The tests were conducted at 200N, 50 Hz frequency, 1 mm stroke length and duration 60 minutes under operating temperature of 80 °C (Fig. 2).

2.5.2 Anti-Wear (AW) Performance of Greases

The four-ball wear test was carried out to investigate the anti-wear property [29]. The steel balls (AISI E52100, 12.7 mm in diameter, RC 65 hardness and Grade 25 Extra Polish, procured from Falex, USA) were used after thoroughly cleaning with hexane prior to experiment runs. Approximately 10 gm of developed grease was utilized for each test run. The AW tests were conducted under different loads (392, 588 and 784 N) with 1200 rpm, at temperature of 75 °C for 60 minutes. In every test, all the four balls were replaced by the new ones. Wear scar diameter (WSD) obtained on the balls was measure using precision optical microscope.

2.5.3 Extreme-Pressure Performance of Grease

The Extreme-pressure (EP) properties of developed grease were evaluated as per modified ASTM D2596. The

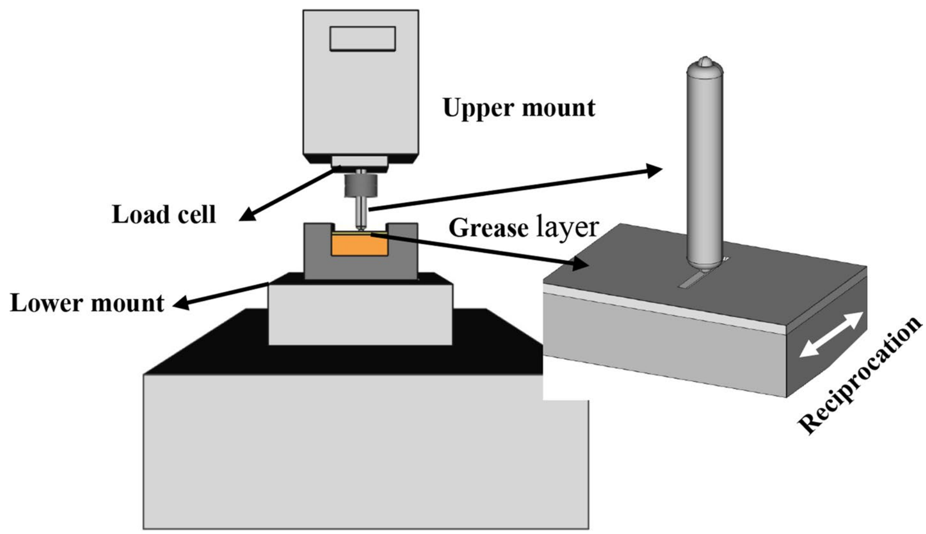

Fig. 2 Schematic layout of UMT reciprocating friction test

operating conditions of EP test were 1760 rpm for 10 s in ambient room temperature conditions. The load was gradually increased till welding of balls or exceeding of WSD beyond 4 mm [30] occurred. The pre-weld load (PWL) a step load lower than obtained weld load (WL) of grease was confirmed by running additional test runs in accordance to ASTM D2596.

2.6 Analysis of Worn Surfaces

Worn surfaces cleaned with acetone and hexane were inspected by using scanning electron microscopy (SEM EVO 10, Carl Zeiss) with Energy dispersion X-ray spectroscopy (EDAX). Raman spectra of graphite particles and worn surfaces AW balls at 784 N were studied using 532 nm wavelength laser on a Renishaw micro-Raman spectrometer (INVIA) using 5 mW laser power with an exposure time of 10 s to enumerate the structure of formed transfer film on the worn tracks.

Also, X-ray photoelectron spectroscopy analysis using (Omicron ESCA), with monochromatic AlKα source was employed to analyse worn surfaces and the peaks of Li, C, Fe, O, were acquired and deconvoluted for further analysis.

3 Results and Discussion

3.1 Characterization of Graphite Particles and Developed Greases

Figure 3 shows TEM and SEM micrograph revealing size and morphology of graphite particles. Figure 3a shows the nano-particles (G_N) as mostly of regular flat shape (Fig. 3a) and average size 50 nm while 450 nm graphite particles (G_S) (Fig. 3b) appear to be flat but with varying sizes and shapes having average size of 430 nm. The medium-sized particles (G_M) in Fig. 3c showed flake irregular-shaped graphite and size around 4 microns. The particles G_B were flake type (platelet) with average size of 10 µm.

The micrographs of frozen nano-grease samples using cryo-SEM are shown in Fig. 4. The detailed procedure of sample preparation procedure for cryo-SEM is reported in the earlier investigation [26]. Cryo-SEMs 4a and 4b are for nano-greases with different magnifications (37,000 and 75,000) and at different locations. Micrograph 4a focused mainly on fibres and NPs sticking on it while micrograph 4b focused on the interior of grease showing homogenous distribution of NPs with marked dimensions. The size of NPs in 4b is almost same as in 4a although magnification is double. The NPs were in de-agglomerated form and their dimensions matched with the dimensions of original NPs. For G_{S4} general appearance at very low magnification (850) is seen in cryo-SEM (Fig. 4c). The sub-micron-sized platelet-shaped particles (G_S) can be seen in frozen grease in micrograph (Fig. 4d) with marked dimensions which match with the original ones.

3.2 Characterization of Greases

Table 4 collects the data for greases on consistency (penetrometer test) and drop point. Addition of graphite particles led to decrease in consistency (i.e. increase in hardness). With decrease in size of particles hardness increased (though the difference was not significant for micro-greases), Nano-greases showed highest hardness values, G_{N4} being the hardest.

Drop point also increased with decrease in size of particles although difference was marginal.

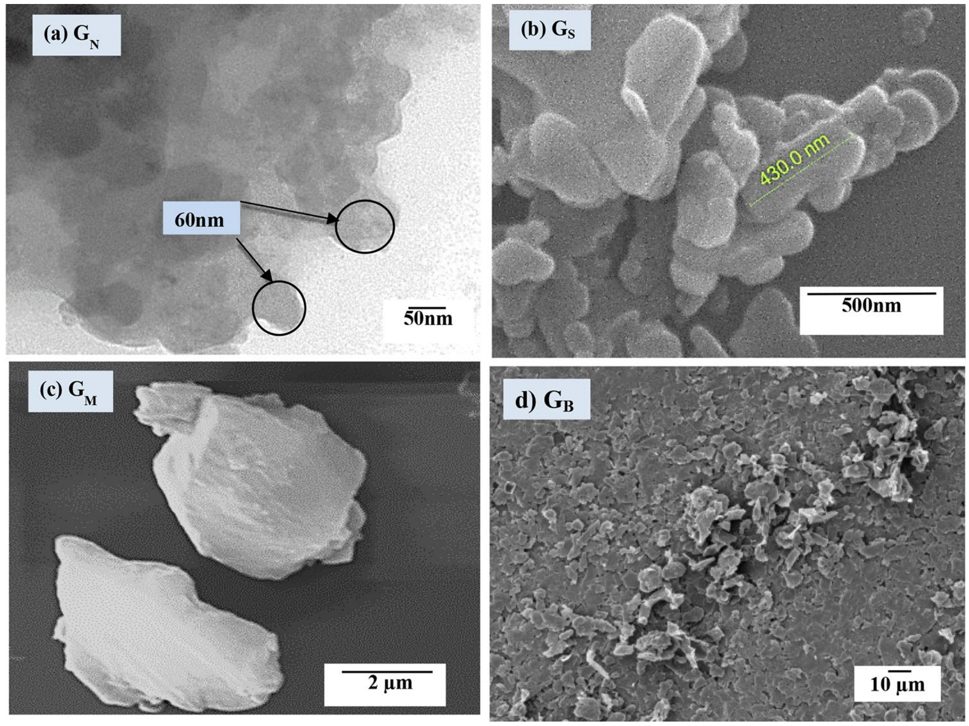

Fig. 3 Micrographs of particles; (**a**) HRTEM (high-resolution transmission electron microscopy) of G_N—Nano-sized; (**b**) FESEM (Field emission scanning electron micrographs) of G_S—sub-micron sized; (**c**) FESEM for G_M—micron sized and (**d**) FESEM for G_B—micron sized

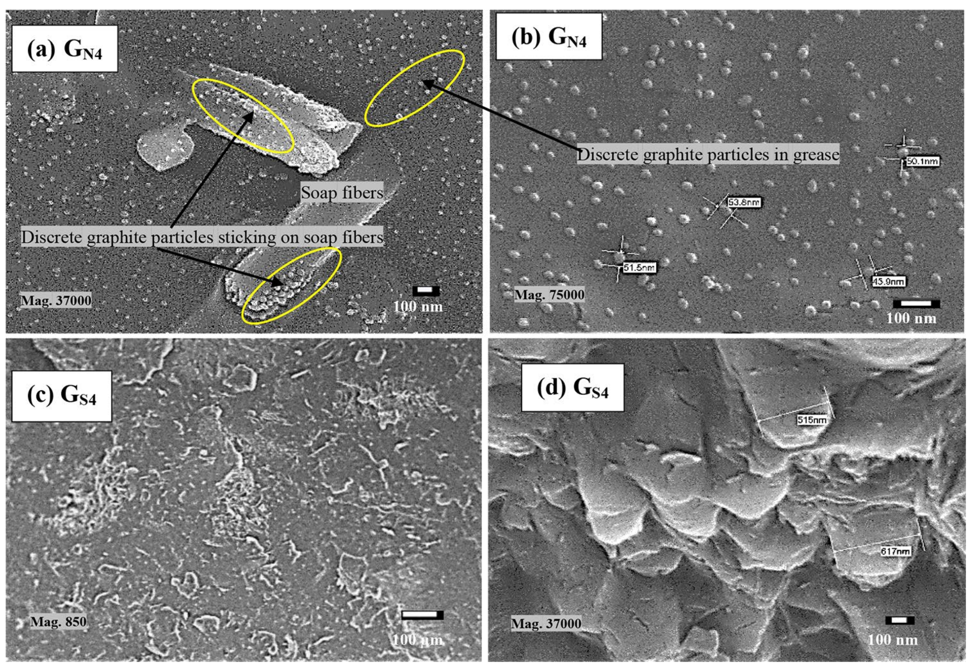

Fig. 4 Cryo-SEM micrographs of (**a** and **b**) nano-grease (G_{N4}) showing soap fibres and distribution of NPs and (**c** and **d**) for G_{S4}

Table 4 Typical grease properties evaluated according to ASTM D1403 and ASTM D217

Grease	Consistency of grease	Drop point (^{0}C)
G_0	410	208
G_{B4}	390	209
G_{M4}	389	210
G_{S4}	385	211
G_{N4}	381	213

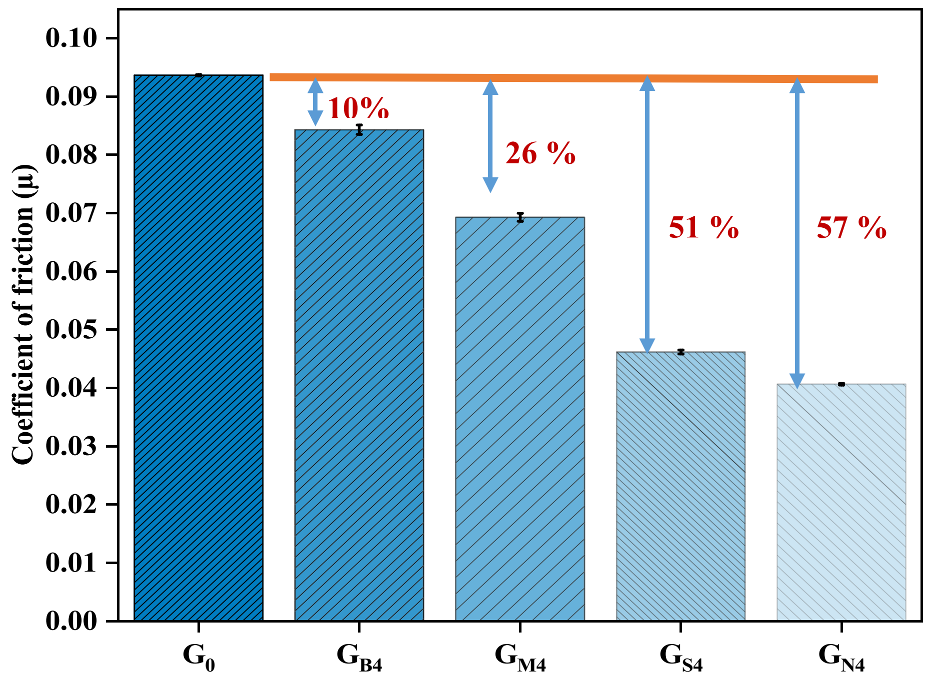

Fig. 5 Coefficient of friction for greases

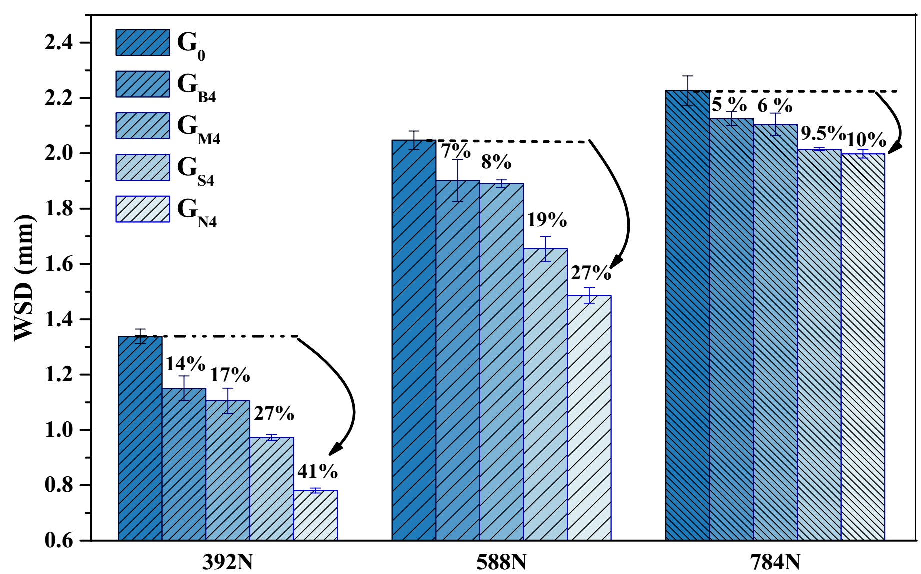

Fig. 6 Effect of loads on the AW performance of grease

3.3 Anti-Friction (AF) Performance of Greases

Figure 5 shows the data on average coefficient of friction from UMT friction test on greases.

Following are the salient observations.

- Doping of graphite particles reduced the friction coefficient of virgin grease significantly
- Lower the size of the particles, higher was the improvement in AF property which could be due to the layer-lattice structure of particles owing to inherent lubricity.

Smaller the size of particles, easier was the interaction with metallic asperities and higher were the benefits. NPs (50 nm and 450 nm) showed significant improvement (50–57%) compared to micro-particles (4–10 micron) (10–26%)

The performance order was G_{N4} (57%) > G_{S4} (51%) > G_{M4} (26%) > G_{B4} (10%) > G_0

3.4 Anti-Wear (AW) Performance of Greases

The anti-wear property of grease was quantified based on WSD (wear scar diameter) formed on the steel balls obtained in AW test. Higher the WSD, higher is the wear tendency and lower is the performance.

Figure 5 shows the WSD data of greases under three different loads (392N, 588N and 784N). The ASTM method prescribes only one load (392N) and tests on additional loads were performed to understand effect of load and possible behaviour under very high loads. Following are the important observations from Fig. 6.

- Inclusion of graphite particles benefitted wear performance although it was load specific and size specific.
- Lower the size, higher were the benefits because of enhanced interaction of smaller particles with metal asperities vis-à-vis formation of a thin and beneficial film on the asperities and tribo-surfaces in contacts.
- Higher the load, lesser were the benefits. At 392 N load, G_{N4} showed maximum enhancement of (41%) in AW compared to G_0. When compared to AF performance, it seems that graphite particles are more beneficial as AF.
- At higher loads, the extent of % improvement as AWA decreased. This was mainly due to the inability of film of graphite particles to sustain the higher loads. This indicates that graphite particles did not have great potential as EPA

3.4.1 Raman Spectroscopy Analysis of Worn Surface

Raman spectra of the pristine graphite NPs, and tribo-films formed on the surfaces of balls worn in G_{N4} and pristine grease were compared. Characteristic D and G peaks of

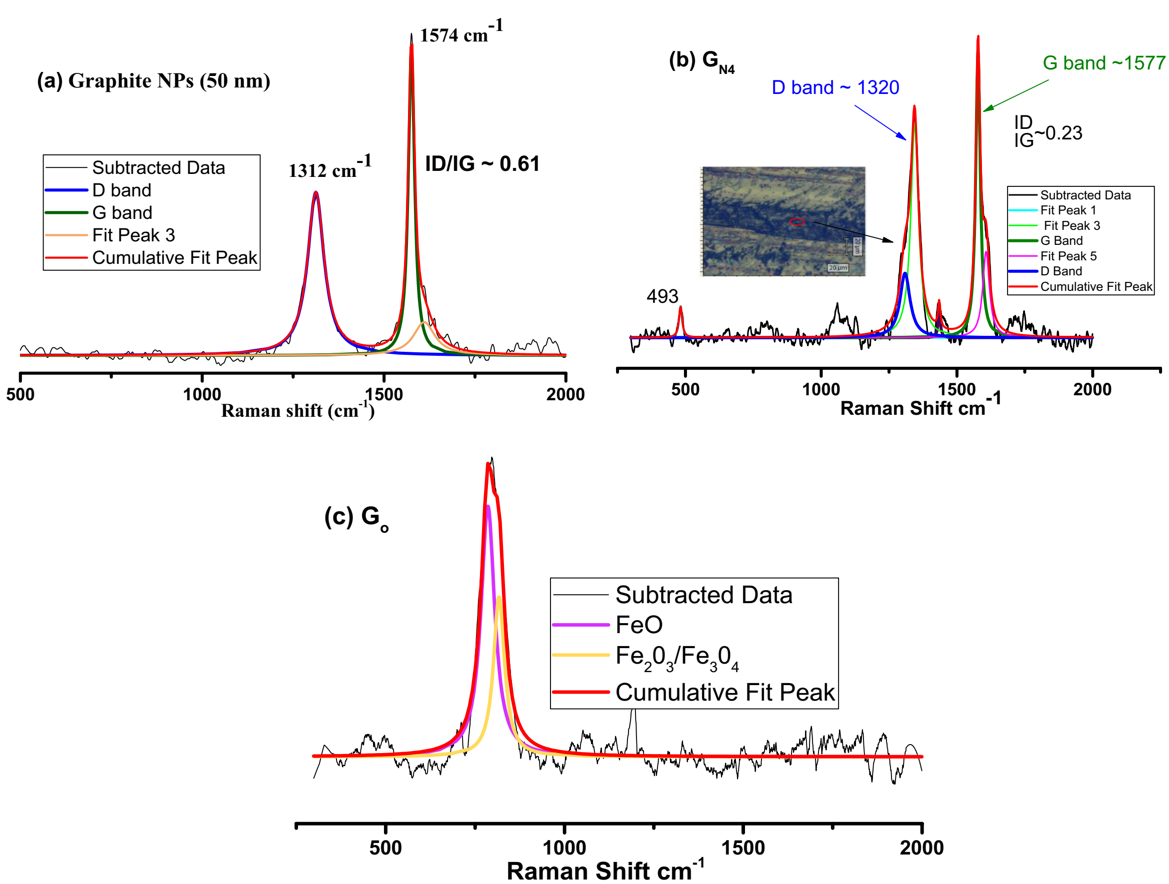

Fig. 7 Raman spectra of (**a**) NPs of graphite (**b**) G_{N4} worn surfaces, (**c**) G_0 worn surfaces measured at 514.5 nm

pristine graphite NPs corresponding to the disorder and order in the graphitic (sp^2 carbon) structure were observed at ~1319 and 1574 cm^{-1}, respectively, as shown in Fig. 7a. Variation in the intensity, width and peak position reveals the possible changes in geometric structure of particles that might have occurred due to shearing stresses during sliding [31–33].

The worn ball surface in pristine grease showed prominent peaks at ~800–1000 cm^{-1}, which are generally assigned to the metallic oxides [33], in particular to iron oxides such as Fe_2O_3, Fe_3O_4 as shown in Fig. 7c. The Raman spectrum on the wear scar of G_{N4} (Fig. 7b) indicates the formation of graphitic tribo-film and a broad peak was observed around 1300–1350 cm^{-1}. Upon deconvolution, two peaks were identified at 1320 and 1348 cm^{-1}. The peak at 1320 cm^{-1} was identified to have originated from the D band of graphitic tribo-film while the peak at 1348 cm^{-1} was attributed of the methyl group of grease [34]. The peak observed at 493 cm^{-1} suggests the presence of iron oxide [33].

Furthermore, in reference to Raman spectrum of Graphite NPs, minor shift in D and G band peaks to a higher Raman wavenumber was detected on the tribo-film of G_{N4} grease-lubricated ball, which might be due to the deformation of NPs under uniaxial compression. The shift in D and G peaks by ~8 and 3 cm^{-1} was observed (1312–1320 cm^{-1} and 1574–1577 cm^{-1}) in the case of G_{N4} ball surface which indicates alteration of C-C (sp^2) structure of graphite NPs due to smearing of particles [32]. This led to the development of deformed carbon tribo-film over the worn surface. More importantly I_D/I_G (the intensity ratio of D to G peak) gives a clear indication for the degree of defects/disorder in the carbon material. The I_D/I_G ratio of pristine nano-graphite was 0.61, while that of film was 0.23, which indicated that the NPs were exfoliated from graphite to graphene over worn tracks due to tribo-stresses during sliding. Similar findings were reported by Xu et al. [33] that the particles in contact zones underwent profound transformation from graphite to graphene sheet on the contact interface due to exfoliation under frictional force. Overall, it can be concluded that graphite NPs were effectively deposited as exfoliated graphitic layer over the wear tracks which were primarily responsible for enhanced anti-wear performance of G_{N4} grease by layering a uniform protective film. Figure 8 shows the conceivable lubrication mechanism of nano-grease enriched with graphite NPs.

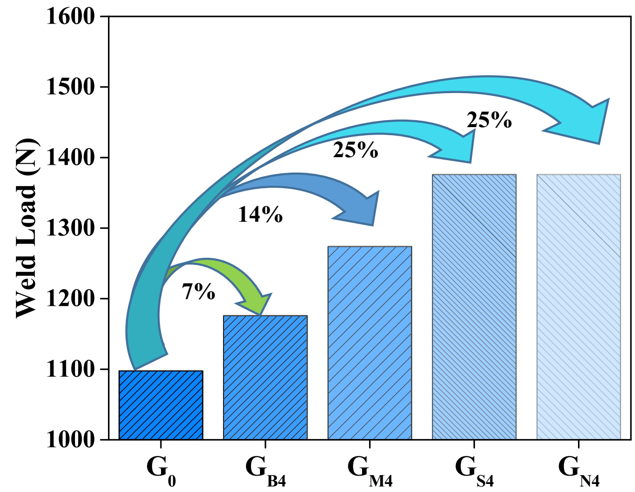

Fig. 9 Size effect of different graphite on EP behaviours of developed nano-greases

3.5 EP Performance Evaluation

The load-carrying capability of any grease can be evaluated using four-ball EP test where higher valve of the WL represents better load-carrying capability and EP performance. Figure 9 showed that nano-sized graphite particles performed extremely better than their micro counterparts with higher weld load. Following was the EP performance trend. The benefits due to particles are not as significant as in AF performance indicating graphite as poor EPA.

$G_{N4} = G_{S4}$ (25%) > G_{M4} (14%) > G_{B4} (7%) > G_0

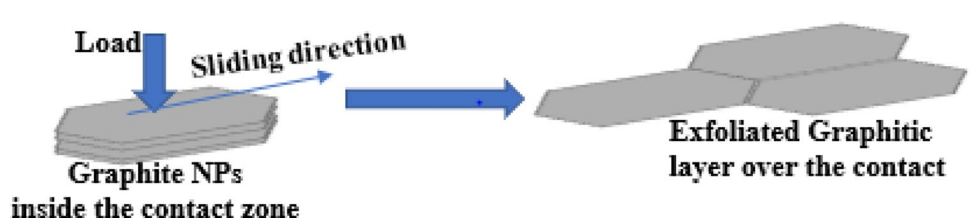

Fig. 8 Schematic showing lubrication mechanism by exfoliation of graphite NPs

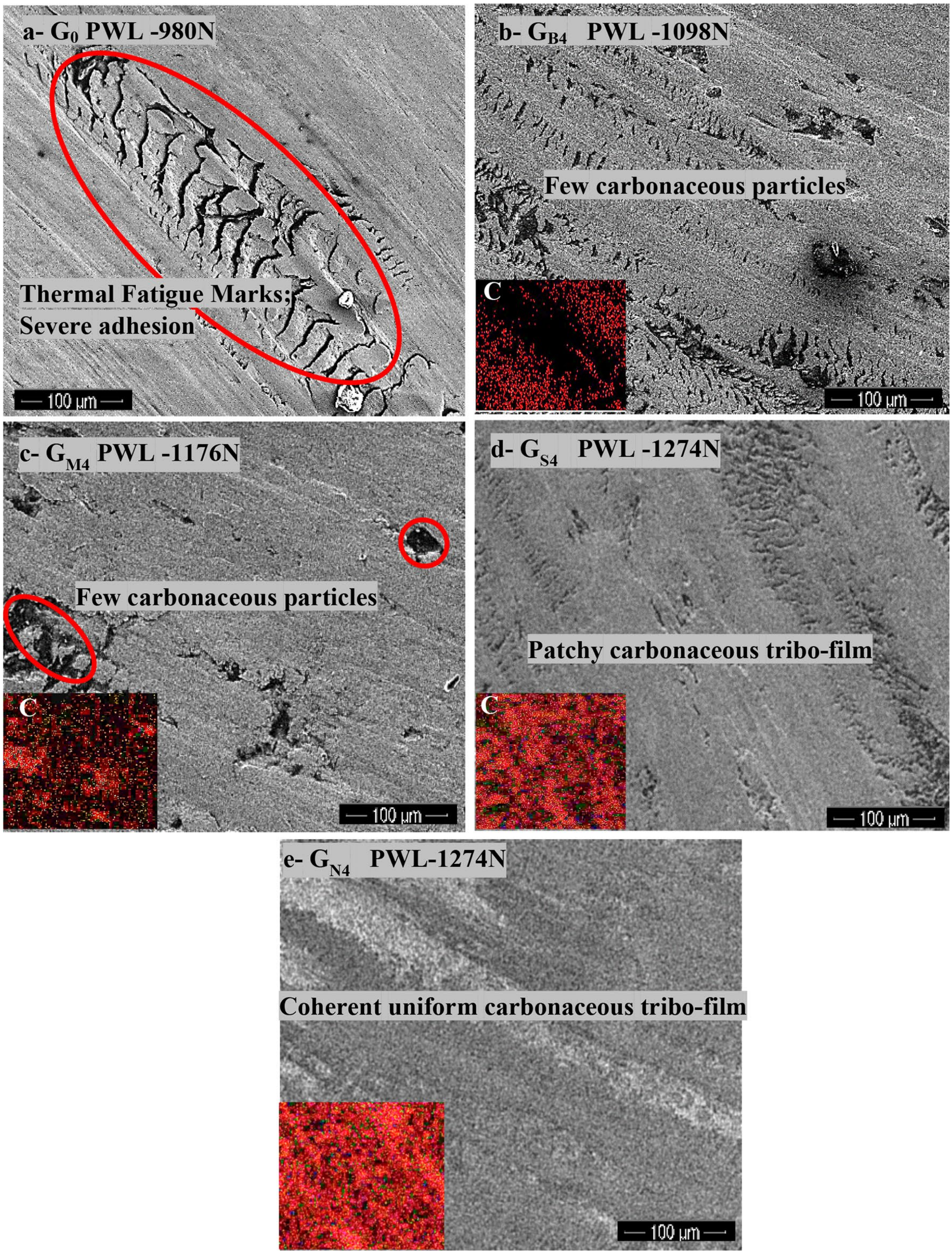

Fig. 10 The SEM micrographs with Carbon dot maps as insets worn surface of PW balls obtained for (**a**) $G_{0,}$ (**b**) G_{B4} (**c**) G_{M4} (**d**) G_{s4} (**e**) G_{N4}

3.5.1 Worn Surface Studies on PW Balls

Figure 10 displays the arranged SEM micrographs of PW balls sequenced in increasing PWL order of grease. The surface without graphite particles (micrograph 10a–980 N PWL) showed the dominating feature of thermal cracks. With inclusion of particles of decreasing size from (micrograph 10b–10d), these cracks sequentially vanished, and surfaces became smoother and smoother confirming being covered with beneficial film of graphite. Micrograph 10e for G_{N4} (highest PWL 1274 N) showed no evidence of such cracks and very smooth surface. Carbon dot map from EDAX data in each micrograph as an inset shows the evidence of graphite film. The density and uniformity of dots were highest in micrograph 10e and the quality deteriorated as moved from micrograph 10e–10b. The Micrograph 10a did not show any C dots since film had no graphite.

3.5.2 XPS Analysis on Pre-Weld Ball Surface

Figure 11 shows the XPS spectra comprising C, O and Fe elements collected from the worn surfaces of pre-weld balls in the selected greases. Significant changes were observed in the intensity of oxygen (O1s) and carbon peaks (C1s) peaks as highlighted in Fig. 11a. Also, the high-resolution spectra obtained for elements O1s and C1s are shown in Fig. 11b, c. It is clearly evident in Fig. 10a, c that G_{N4} ball surface had the highest intense C1s peak (i.e. highest content of Carbon/graphite). On the other hand, G_{N4} ball surface showed lowest intensity O1s peak (lowest O content and lowest oxidation). This confirmed that added graphite NPs prevented the oxidation of ball surface to the maximum extent. The O1s binding energies at 530.1 and 531.5 eV in particularly are assigned to metal oxides and hydroxides present at the stainless-steel surface [14, 35]. The deconvoluted C1s spectra of the sample lubricated with virgin grease (Fig. 11d), showed a peak around ~285.3 eV which might be attributed to the C-O bond [36]. This observed C-O bond was mainly due to oxidation of the added oil additives and parent oil. While deconvoluted C 1s peak of nano-grease showed peaks at ~282.4 eV, which was attributed to the aliphatic carbon C-C (sp2) bonds. Thus, it is conclusive that G_{N4} formed better carbon enriched tribo-film onto ball surface that acted as anti-wear and prevented further oxidation of ball surface. The studies also confirmed that the graphite had no capability to chemically react with the metal surface and build chemically modified layer imparting high EP property.

4 Conclusions

Following conclusions were drawn based on the outcome of the study on investigating the influence of variation in size of graphite particles including nano-particles on the tribo-performance of grease. $G_{N4,}$ G_{S4}, G_{S4} and G_{B4} greases contained 4 wt. % graphite particles of 50 nm, 450 nm, 4 micron and 10 micron, respectively, and G_0 was a virgin grease without any particles. Overall, it was concluded inclusion of graphite particles proved beneficial for improving all the selected categories such as anti-friction, anti-wear and extreme-pressure performance, although the extent of highest benefits were category specific. Graphite particles proved most effective as anti-friction additive (AFA), followed by anti-wear additive (AWA) and then as extreme-pressure additive (EPA). In each category, smaller the size of graphite particles, better was the performance of filled greases. Following were the major trends in performance:

- As AFA – G_{N4} (57%) >G_{S4} (51%) > G_{S4} (26%) > G_{B4} (10%) >G_0
- As AWA,
  - 392N load: G_{N4} (41%) > G_{S4} (27%) > G_{M4} (17%) >G_{B4} (14%)>G_0
  - 588N load: G_{N4} (27%) > G_{S4} (19%) > G_{M4} (8%) >G_{B4} (7%)>G_0
  - 784N load: G_{N4} (10%) > G_{S4} (9.5%) >G_{M4} (5.5%) >G_{B4} (4.5%)>G_0

It was also concluded that benefits as AWA were load specific. Higher the load, lesser were the benefits.

- As EPA- G_{N4} (25%) ≥ G_{S4} (25%) > GM_4 (14%) > G_{B4} (7%) > G_0

The SEM-EDAX studies on pre-weld balls confirmed the graphite film of better and better quality with decreasing size of particles was responsible for the improved performance. Based on the XPS studies, it was also concluded that the film was not chemically modified during EPA test, which was the reason for its poor EP potential. Improvement (≈25%) for nano-grease was due to reduced extent of oxidation of the steel surface as a consequence of physically formed graphite film of very good quality on the ball surface.

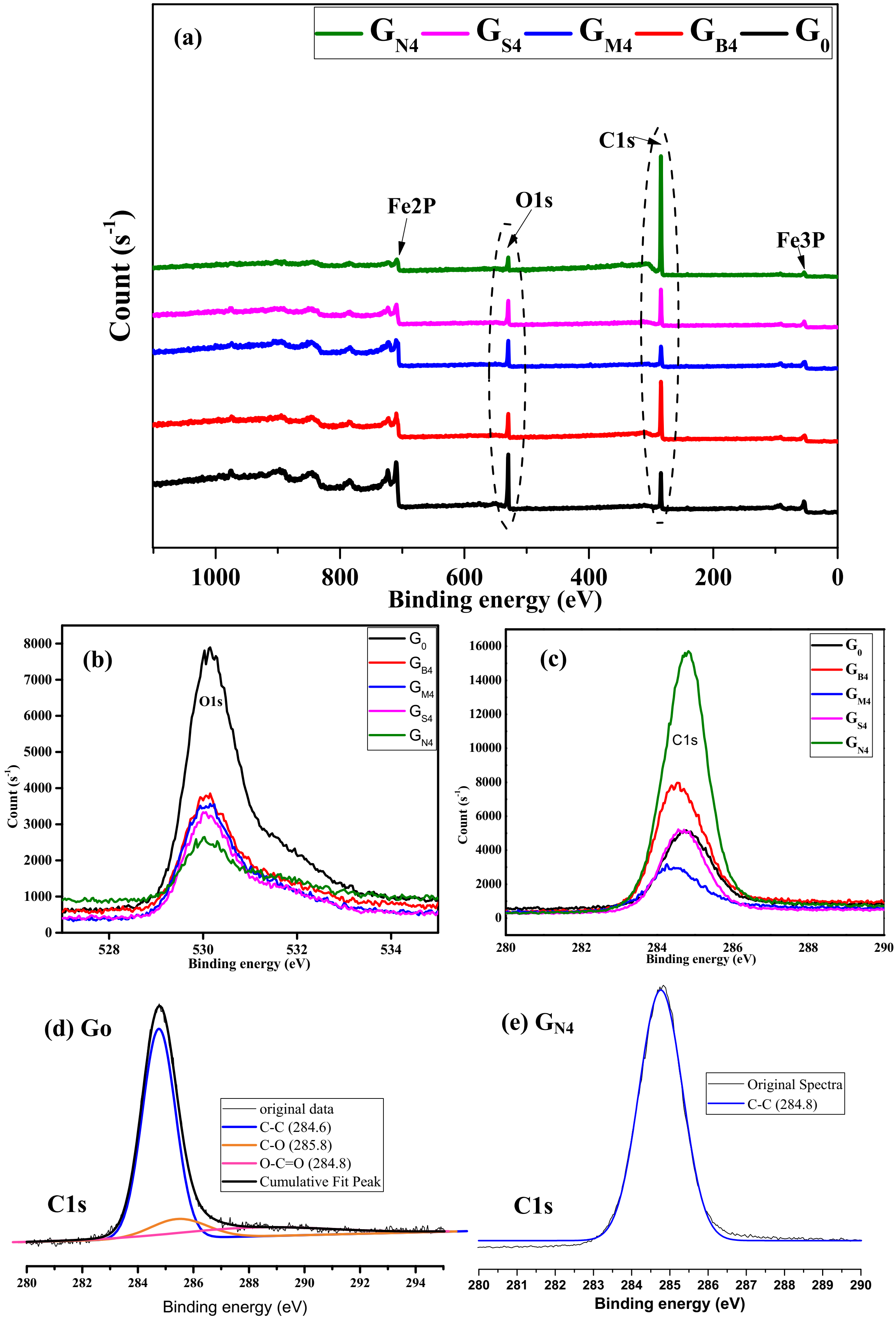
(a)
GN4
GS4
GM4
GB4
G0
C1s
O1s
Fe2P
Fe3P
Count (s-1)
1000
800
600
400
200
0
Binding energy (eV)
(b)
O1s
G0
GB4
GM4
GS4
GN4
Count (s-1)
Binding energy (eV)
(c)
C1s
Count (s-1)
Binding energy (eV)
(d) Go
C1s
original data
C-C (284.6)
C-O (285.8)
O-C=O (284.8)
Cumulative Fit Peak
Binding energy (eV)
(e) GN4
C1s
Original Spectra
C-C (284.8)
Binding energy (eV)

◂**Fig. 11** XPS spectroscopy analysis on transfer films formed on PW balls (**a**); overall spectra (**b**); spectrum for O1s (**c**); spectrum for C1s; and Deconvoluted spectrum of C1s of (**d**) pristine grease (Go), (**e**) G_{N4} ball surface

References

1. Holmberg, K., Erdemir, A.: Influence of tribology on global energy consumption, costs and emissions. Friction. **5**, 263–284 (2017)
2. Holmberg, K., Erdemir, A.: The impact of tribology on energy use and CO_2 emission globally and in combustion engine and electric cars. Tribol. Int. **135**, 389–396 (2019)
3. Spikes, H.: Friction modifier additives. Tribol. Lett. **60**, 5 (2015)
4. Kotia, A., Borkakoti, S., Ghosh, S.K.: Wear and performance analysis of a 4-stroke diesel engine employing nanolubricants. Particuology. **37**, 54–63 (2018)
5. Saini, V., Bijwe, J., Seth, S., Ramakumar, S.S.V.: Role of base oils in developing extreme pressure lubricants by exploring nano-PTFE particles. Tribol. Int. **143**, 106071 (2020)
6. Spikes, H.: Stress-augmented thermal activation: Tribology feels the force. Friction. **6**, 1–31 (2018)
7. Jianbin, L., Zhou, X.: Superlubricitive engineering—Future industry nearly getting rid of wear and frictional energy consumption. Friction. **8**, 643–665 (2020)
8. Stolarski, T., Olszewski, O.: An experimental study of the frictional mechanism in a journal bearing lubricated with grease containing powdered PTFE. Wear. **39**, 377–387 (1976)
9. Jiguo, C.: Tribological properties of polytetrafluoroethylene as additive in titanium complex grease. Ind. Lubr. Tribol. **64**, 98–103 (2012)
10. Palios, S., Cann, P.M., Spikes, H.A.: Behaviour of PTFE suspensions in rolling/sliding contacts. Tribol. Ser. **31**, 141–152 (1996)
11. Sahoo, R.R., Biswas, S.K.: Effect of layered MoS_2 nanoparticles on the frictional behavior and microstructure of lubricating greases. Tribol. Lett. **53**, 157–171 (2014)
12. Silver, H.B., Stanley, I.R.: The effect of the thickener on the efficiency of load-carrying additives in greases. Tribology. **7**, 113–118 (1974)
13. Niu, M., Qu, J.: Tribological properties of nano-graphite as an additive in mixed oil-based titanium complex grease. RSC Adv. **8**, 42133–42144 (2018)
14. Saini, V., Bijwe, J., Seth, S., Ramakumar, S.S.V.: Potential exploration of nano-talc particles for enhancing the anti-wear and extreme pressure performance of oil. Tribol. Int. **151**, 106452 (2020)
15. Wang, L., Wang, B., Wang, X., Liu, W.: Tribological investigation of CaF_2 nanocrystals as grease additives. Tribol. Int. **40**, 1179–1185 (2007)
16. Ji, X., Chen, Y., Zhao, G., Wang, X., Liu, W.: Tribological properties of $CaCO_3$ nanoparticles as an additive in lithium grease. Tribol. Lett. **41**, 113–119 (2011)
17. Krawiec, S.: The synergistic effect of copper powder with PTFE in a grease lubricant under mixed friction conditions. Arch. Civil Mech. Eng. **11**, 379–390 (2011)
18. Zheng, B., Zhou, J., Jia, X., He, Q.: Friction and wear property of lithium grease contained with copper oxide nanoparticles. Appl. Nanosci. **10**, 1355–1367 (2020)
19. Cheng, Z.L., Qin, X.X.: Study on friction performance of graphene-based semi-solid grease. Chin. Chem. Lett. **25**, 1305–1307 (2014)
20. Fan, X., Xia, Y., Wang, L., Li, W.: Multilayer graphene as a lubricating additive in bentone grease. Letters. **55**, 455–464 (2014)
21. Mohamed, A., Osman, T.A., Khattab, A., Zaki, M.: Tribological behavior of carbon nanotubes as an additive on lithium grease. J. Tribol. **137**, 011801 (2015)
22. Al-Saadi, D.A.Y., Pershin, V.F., Salimov, B.N., Montaev, S.A.: Modification of graphite greases graphene nanostructures. J. Frict. Wear. **38**, 355–358 (2017)
23. Rawat, S.S., Harsha, A.P., Chouhan, A., Khatri, O.P.: Effect of graphene-based nanoadditives on the tribological and rheological performance of paraffin grease. J. Mater. Eng. Perform. 4, 1–13 (2020)
24. Mohammed, M.A.: Effect of additives on the properties of different types of greases. Iraqi J. Chem. Pet. Eng. **14**, 11–21 (2013)
25. Li, Z., He, Q., Du, S., Zhang, Y.: Effect of few layer graphene additive on the tribological properties of lithium grease. Lubr. Sci. **32**(7), 333–343 (2020)
26. Kumar, N., Saini, V., Bijwe, J.: Performance properties of lithium greases with PTFE particles as additive: Controlling parameter-size or shape? Tribol. Int. **148**, 106302 (2020)
27. Gupta, M.K., Bijwe, J.: Exploration of potential of graphite particles with varying sizes as EPA and AWA in oils. Tribol. Int. **127**, 264–275 (2018)
28. Wang, H., Wang, Y., Liu, Y., Zhao, J., Li, J., Wang, Q., Luo, J.: Tribological behavior of layered double hydroxides with various chemical compositions and morphologies as grease additives. Friction. https://doi.org/10.1007/s40544-020-0380-5 (2020)
29. ASTM International 2015 ASTM D2266 Standard Test Method for Wear Preventive Characteristics of Lubricating Grease (Four-Ball Method)
30. ASTM International 2015 ASTM D2596 Standard Test Method for Measurement of Extreme-Pressure Properties of Lubricating Grease (Four-Ball Method)
31. Ferrari, A.C.: Raman spectroscopy of graphene and graphite: Disorder, electron–phonon coupling, doping and nonadiabatic effects. Solid State Commun. **143**, 47–57 (2007)
32. Gupta, M.K., Bijwe, J., Kadiyala, A.K.: Tribo-investigations on oils with dispersants and hexagonal boron nitride particles. J. Tribol. **140** (2018)
33. Xu, Y., Geng, J., Zheng, X., Dearn, K.D., Hu, X.: Friction-induced transformation from graphite dispersed in esterified bio-oil to grapheme. Tribol. Lett. **63**, 18 (2016)
34. Sahoo, R.R., Biswas, S.K.: Effect of layered MoS_2 nanoparticles on the frictional behaviour and microstructure of lubricating greases. Tribol. Lett. **53**, 157–171 (2014)
35. Nesbitt, H.W., Scaini, M., Hochst, H., Bancroft, G.M., Schaufuss, A.G., Szargan, R.: Synchrotron XPS evidence for Fe2+-S and Fe3+-S surface species on pyrite fracture-surfaces, and their 3D electronic states. Am. Mineral. **85**, 850–857 (2000)
36. Paul, G., Shit, S., Hirani, H., Kuila, T., Murmu, N.C.: Tribological behavior of dodecylamine functionalized graphene nanosheets dispersed engine oil nanolubricants. Tribol. Int. **131**, 605–619 (2019)